npj | women's health

Article

https://doi.org/10.1038/s44294-025-00088-6

Low-cost fiber-based electrochemical sensor for quantification of acetaminophen in human breast milk

Check for updates

Mona A. Mohamed [1,5], Melissa Banks [1,5], Sina Khazaee Nejad [1], Abdulrahman Al-Shami [1], Ali Soleimani [1], Haozheng Ma [1], Farbod Amirghasemi [1], Victor Ong [1] & Maral P. S. Mousavi [1,2,3,4] ✉

Acetaminophen is the most common cause of acute liver failure in the United States. The transfer of drugs to breast milk poses risks to infants, yet dosing guidelines are based on limited data from small studies. Currently, drug levels in milk are simply estimated through invasive blood draws. We present a new low-cost, textile-based electrochemical sensor for detecting acetaminophen at the point of use in breast milk. An embroidered conductive yarn (steel and silver) is used, which eliminates the need for complex microfabrication processes. A gold-nanoparticle-doped carbon ink-modified steel yarn serves as the working electrode, with pristine steel and silver yarns as counter and reference electrodes, respectively. Using square wave voltammetry, the sensor achieves a linear detection range of 9.9–166.4 μM in undiluted breast milk, with a limit of detection of 1.15 μM. This platform provides a simple and accessible alternative for drug monitoring

Acetaminophen has been approved by the US Food and Drug Administration for over-the-counter use since 1955[1]. The drug gained popularity in the early 1980's when concerns arose that aspirin use was linked to the development of Reye's syndrome in children[2]. Acetaminophen, also known as paracetamol outside of the US and Japan, is also sold under the brand name Tylenol. Despite its ubiquity, the exact mechanism of action by which acetaminophen blocks pain has yet to be fully understood[3].

While many have used acetaminophen safely, many others have suffered severe consequences as a result of overexposure to the drug (Fig. 1 shows the common side effects). Acetaminophen toxicity results in over 56,000 emergency room visits each year, with incidence increasing over the past decade[4,5]. Regardless of its status as a medicine cabinet staple, the drug remains the most common cause of acute liver failure in children, as well as the most common cause of liver transplantation in the United States[6–8]. The American Academy of Pediatrics does not recommend the use of acetaminophen in patients under 3 months of age without clinical supervision[9], yet it remains one of the most commonly administered medications for children and neonates[10]. Adding to the concern is the fact that acetaminophen is the most commonly prescribed drug for managing maternal postpartum pain after both vaginal and cesarean births[11]. Medications consumed by the lactating mother are secreted in breast milk to varying degrees (Fig. 1A), depending on the hydrophobicity and molecular weight of the drug, and the volume of milk produced. These pharmaceuticals are then consumed by the nursing infant, potentially resulting in a cumulative hepatotoxic effect. As the child's liver struggles to process indirect, and potentially direct, acetaminophen exposure, they can sustain hepatocellular liver injury, which can result in acute liver failure with or without coagulopathy[12].

Before a medication can be secreted in breast milk, it must first enter the systemic circulation of the mother. Upon administration, acetaminophen is primarily metabolized in the liver with some assistance provided by the kidneys and intestine[13]. Once metabolized, the drug enters the bloodstream where it eventually passes through mammary capillaries and into mammary tissue. Because pharmacokinetics are dependent on person-specific factors such as height, weight, sex, metabolism, comorbidities, and genetics, drug plasma levels vary across subjects despite consistent dosage[14–18]. Once the drug is delivered to mammary tissues, it enters breast milk through three different modalities: active transport, passive diffusion, or apocrine secretion[19]. The degree to which the medication is secreted in breast milk is determined by multiple parameters including its lipid

[1]Alfred E. Mann Department of Biomedical Engineering, University of Southern California, Los Angeles, CA, USA. [2]Department of Chemistry, University of Southern California, Los Angeles, California, 90089, USA. [3]Department of Psychiatry and Behavioral Sciences, University of Southern California, Los Angeles, California, 90033, USA. [4] Department of Pharmacology and Pharmaceutical Sciences, Alfred E. Mann School of Pharmacy and Pharmaceutical Science, University of Southern California, Los Angeles, California, 90033, USA. [5]These authors contributed equally: Mona A. Mohamed, Melissa Banks.
✉e-mail: mousavi.maral@usc.edu

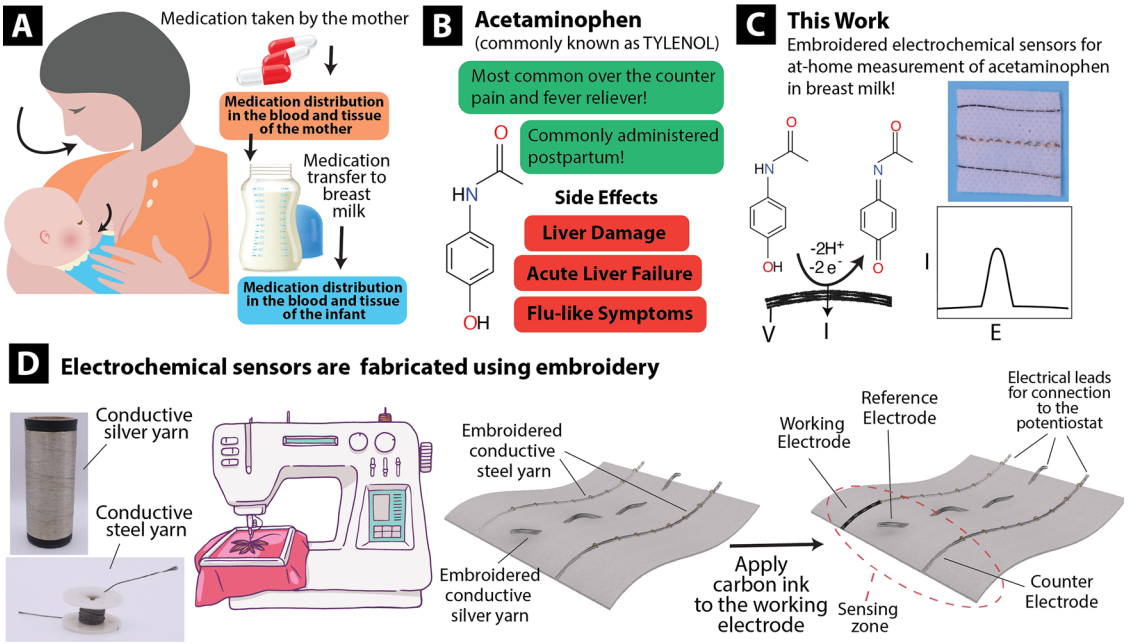

Fig. 1 | Overview of the work. A Systemic progression of drug absorption and excretion into breast milk.**B** Molecular structure and potential side effects of acetaminophen toxicity. **C** Oxidation of acetaminophen at the surface of embroidered electrodes results in electrical current which is detected at the working electrode, and used to quantify the concentration of acetaminophen in solution. A photo of the electrodes on a textile backing. **D** Fabrication and surface modification of embroidered electrodes, and starting conductive fibers of steel, and silver-plated polypropylene fiber.

solubility, degree of ionization, and mechanism of transport[18–20]. Once the drug has been metabolized, there exists a direct relationship between the concentration of the drug in the blood plasma and expressed milk. This relationship is referred to as the milk-to-plasma ratio (m/p); the higher the ratio, the more of the drug secreted into breast milk. Drugs transferred to the child through their mother's milk place (potentially compounding) stress on the infant's liver and excretory system 1B. This indirect exposure to medications through breast milk is not currently quantified. As such, mothers are left with a difficult decision to expose their infants to the medication while nursing, refrain from taking the pain-killer and exposing themselves to pain and discomfort, or forego breast milk entirely and opt to formula-feed for an indefinite period of time. By monitoring maternal drug output in breast milk, healthcare providers can more accurately calculate therapeutic dosages for both baby and mother.

There are no tools for at-home or point-of-use quantification of acetaminophen in breast milk. Traditional methods of maternal drug quantification use blood draws to measure drug plasma concentration[18–20]. The drug concentration is then estimated based on the its m/p ratio (if known). Frequent blood draws are painful, costly (due to necessary doctor appointments and laboratory fees), and inconvenient. The common method of detection in the case of acetaminophen is liquid chromatography coupled with mass spectrometry[17]. This technique requires expensive and bulky equipment, hazardous chemical solvents that should only be used in a laboratory setting, and skilled operators, which are all clearly incompatible with an at-home or point-of-care use.

If the m/p ratio is not reported, it is calculated by simultaneously measuring drug concentration in the blood and milk of lactating volunteers. It is important to note that the m/p ratio suffers from multiple limitations. As metabolic rates vary from person to person, the resultant drug concentrations at a particular point in time will likewise vary[15]. There is also the issue of dilution between nursing sessions. As breast milk is continually secreted throughout the day and stored in the mammary alveoli, resultant concentrations will change as more or less drug is secreted based on maternal dosing[18,20]. As a result of these variations, different m/p ratios are reported for the same drug. For example, Abduljalil et al. reported a m/p ratio of 0.83 (measured from 10 subjects)[20], while others reported m/p ratios of 0.94 (eight subjects)[21], 1.05 (number of subjects not specified[16], and 0.76 (three lactating subjects)[22]. The observed discrepancies in reported m/p ratios necessitate personalized and frequent monitoring of acetaminophen levels directly in breast milk. This approach is essential to fully capture inter-individual variations and intra-individual changes throughout the lactation period.

In this work, we have developed a low-cost, textile-based, electrochemical platform for the at-home or point-of-care detection of acetaminophen in whole undiluted human breast milk. Our platform measures acetaminophen based on the drug's inherent electrochemical properties and its oxidation at the surface of an electrode. Electrochemical activity of acetaminophen has been shown in other works on a wide range of electrochemical systems and materials, and acetaminophen has been measured electrochemically in various biofluids, including human-derived bodily fluids such as serum, urine, sweat, and saliva[23–26]. To the best of our knowledge, this work reports the first electrochemical measurement of acetaminophen in human breast milk (regardless of the sensing platform and materials and methods used for sensor fabrication). We developed our sensor by embroidering cost-effective conductive steel and silver fibers onto a textile backing, resulting in a flexible and inexpensive sensor. The use of yarn and thread in developing electrochemical sensors offers several significant advantages. These materials are inexpensive, lightweight, flexible, and mechanically robust, making them ideal for creating wearable and portable sensing devices. Their fibrous and porous structures provide a high surface area, which enhances the loading of active materials and improves sensor sensitivity. Additionally, yarns and threads can be easily functionalized with conductive materials, enzymes, or other sensing elements, enabling diverse electrochemical sensing applications[27–34].

The emerging research on fabricating sensors from textiles and conductive fibers has shown significant potential through the integration of conductive nanomaterials and the incorporation of conductive fibers using traditional techniques like knitting, weaving, and embroidery[27,31,35–41]. While there is a substantial amount of research on using conductive fibers to develop electrodes for electromyography and electrocardiography, there is comparatively less work on applying these embroidered electrodes for electrochemical detection[42–44]. Of the latter, coated/plated yarns (typically

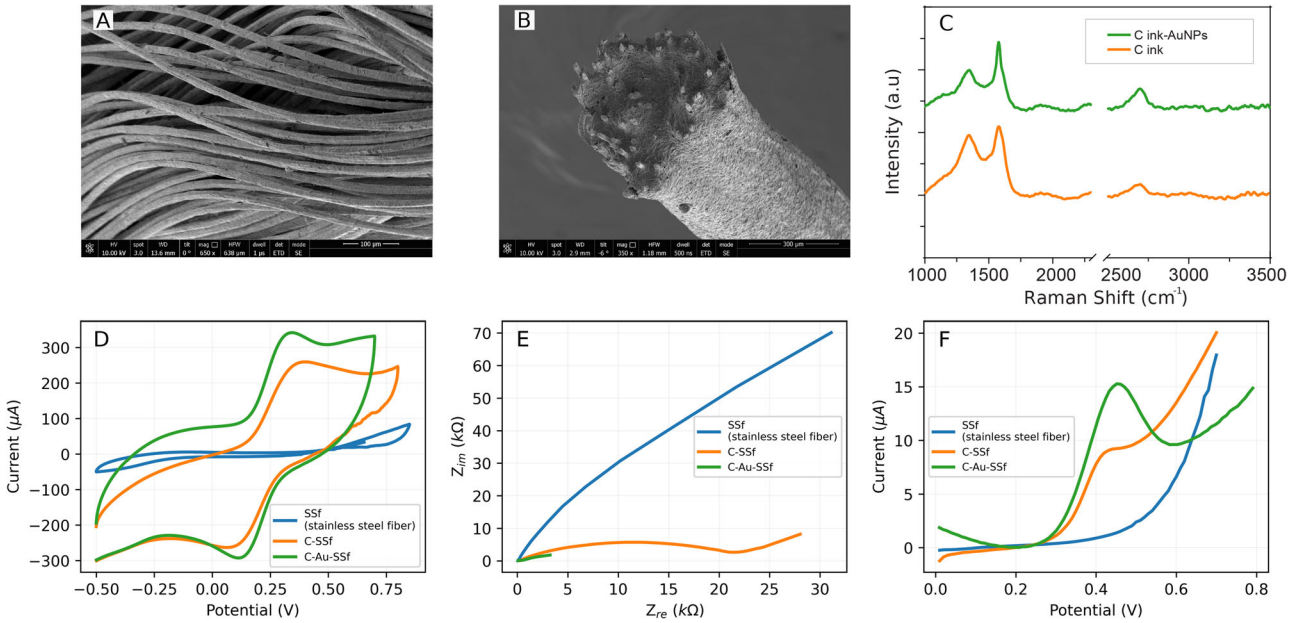

Fig. 2 | Characterization of yarn-based sensors. A shows the SEM of the steel yarn, measured without any additional conductive coatings. **B** shows the SEM of C-Au-SSf. **C** shows the Raman Spectra for carbon ink and carbon ink doped with AuNPs. **D** demonstrates CVs of pristine and modified SSf in 5 mM $[Fe(CN)_6]^{3-/4-}$ and 100 mM KCl. **E** shows the electrochemical impedance spectra (EIS) of pristine and modified SSf, measured in 5 mM $[Fe(CN)_6]^{3-/4-}$ and 100 mM KCl. SWV of 74 μM of acetaminophen in pH 7 buffer, measured with pristine and modified SSf. An external Ag-AgCl reference electrode and a Pt wire as counter electrode were used for electrochemical measurements.

gold, carbon inks, or conductive polymer) are popular, having been used to develop enzyme-based electrochemical sensors for glucose, lactate, and uric acid, as well as non-enzymatic detection of hemoglobin[32,35,45–50]. Less common is the use of a naturally-conductive thread material such as carbon nanotube fibers and stainless steel[51,52]. To the best of our knowledge, this is the first report of an electrochemical sensor fabricated from this low-cost steel fiber. The flexible electrochemical sensing system developed in our work can directly measure the concentration of acetaminophen in milk, eliminating the error associated with the use of a one-size-fits-all m/p ratio.

By creating a platform that directly measures drug output in milk, we allow lactating parents to manage their pain and their infant's health more effectively. Direct measurement also removes the need for mothers to document exact time of medication administration and subsequent nursing or pumping session to estimate their level of drug secretion. Additionally, this technology can further efforts in large-scale drug measurements in donated breast milk at milk banks. There are very few tools available for analysis of breast milk, and we hope this work will address the technology gap for at-home and point-of-care analyses for women's health.

Results

Acetaminophen can be directly detected via oxidation at the surface of a working electrode[23–26,53]. Through the development of appropriate electrode materials and electrochemical sensing platforms, we hypothesized that acetaminophen could be measured in breast milk. We aimed to develop a robust detection platform that can be adapted for point-of-care quantification and, in the future, for the development of wearable sensors. We started our work by looking into low-cost conductive fibers and mostly found copper and silver-plated yarns. Despite their excellent electrical conductivity, the high electroactivity and low oxidation potential of silver and copper make them unsuitable as working electrodes for voltammetric or amperometric analyses. We came across a low-cost steel fiber (available through Adafruit) with outstanding conductivity (less than 10 Ohm per feet) and mechanical strength. While these fibers have been used in other works in limited settings for electrical connections in wearable devices and for the development of super capacitors[54,55], the electrochemical properties of this material for sensing have not been studied. Moreover, the application of this steel fiber for electrochemical sensing has not been explored.

Noteworthy, the steel fiber is conductive to the core and not plated over a non-conductive backbone, resulting in outstanding mechanical properties and high resilience. Figure 2 shows the scanning electron microscopy (SEM) image of this fiber (pristine fiber without any metal coatings), demonstrating a network of 13.8 ± 0.8 μm fibers twisted together to form a 700 ± 33 μm thick conductive fiber bundle. We observed no changes in steel fiber conductivity aftermultiple connections and disconnections with an alligator clip. However, for silver and copper-plated fibers, we noted metal delamination and high contact resistance. In this work, we first study the electrochemical properties of the steel fiber as a working electrode for the measurement of acetaminophen in breast milk, we then explore the sensitivity and selectivity of the working electrode using an external counter and reference electrode. Finally, we integrate a fully fiber-based embroidered sensing system onto a textile backing.

The bare steel fiber has poor electro-catalytic activity, as demonstrated in Fig. 2D where no peaks are observed in the cyclic voltammogram of the well-established ferrocyanide-ferricyanide redox couple. This low electrochemical activity for steel is known and is likely caused by the presence of passivating oxide coatings[56]. To address this issue, we utilized the pristine stainless steel fiber (SSf) for electrical connections (i.e., SSf acts a flexible wire), and modified the surface of SSf with conductive carbon-based and nano-particle (NP) based inks to enhance electrocatalytic activity for voltammetric analysis of acetaminophen. To evaluate effective materials for surface modification, we cut the steel fiber to 7 cm pieces, and coated one end with a commercial graphite carbon ink that was doped with doped with (1) gold nanoparticles (AuNP), (2) graphene oxide (GO), and (3) multi-walled carbon nanotubes (MWCNT). Cyclic voltammographs of ferrocyanide-ferricyanide redox couple was measured with this modified SSf (external reference and counter electrode) to identify the most effective ink composition and evaluate electrode surface area. We also measured square wave voltammograms (SWV) of acetaminophen with the modified SSf to determine the ink composition that has the most catalytic activity for the oxidation of acetaminophen. As shown in Supplementary Fig. 1, AuNPs had

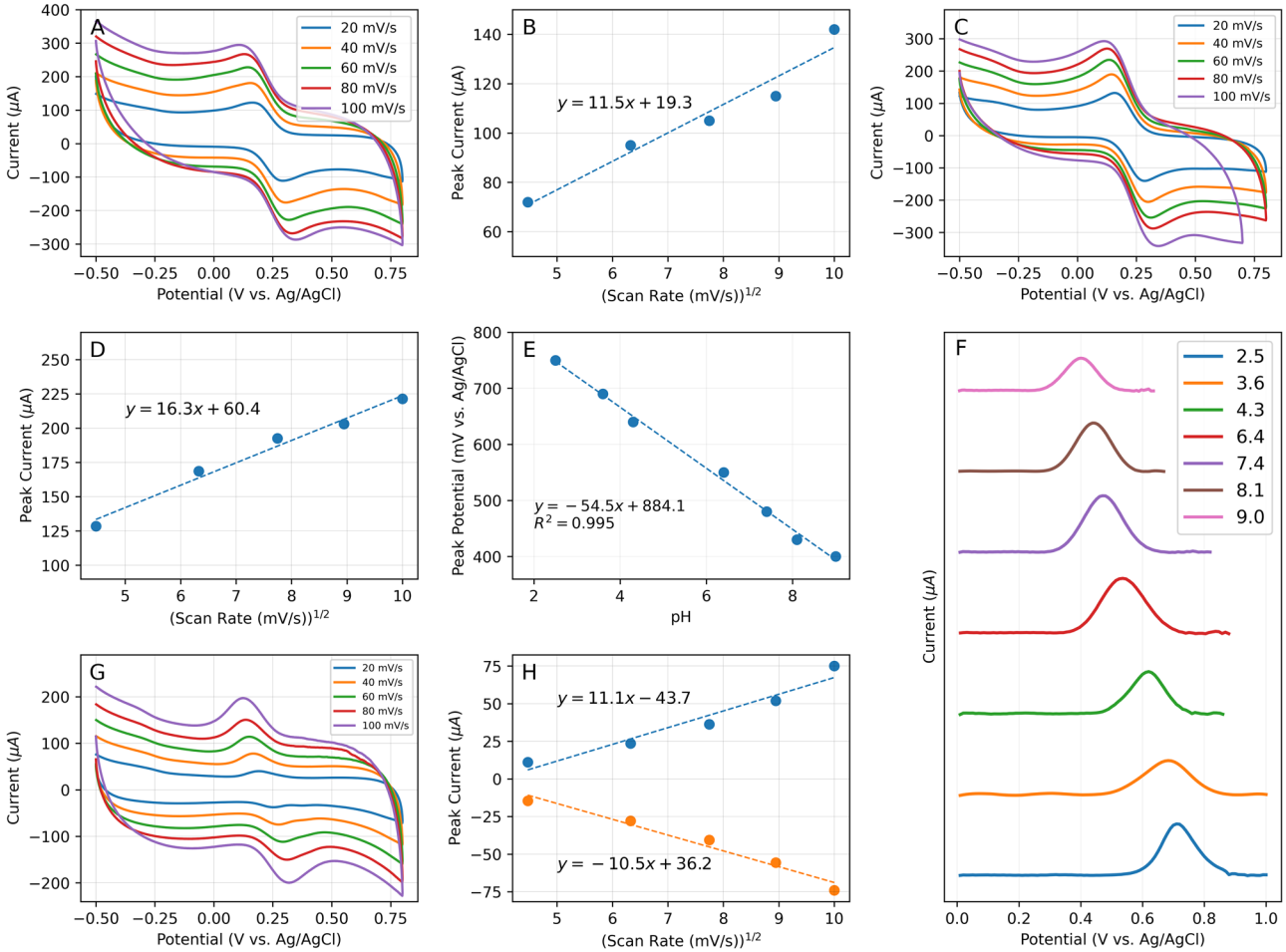

Fig. 3 | Electrochemical characterization. A CVs of C-SSf in 5.0 mM $[Fe(CN)_6]^{3-,4-}$ at different scan rates. **B** Peak current (I_p) of CVs measured in A plotted vs. the square root of the scan rate. **C** CVs of C-AuNP-SSf in 5.0 mM $[Fe(CN)_6]^{3-,4-}$ at different scan rates. **D** I_p of CVs measured in D plotted vs. square root of the scan rate. **E** Peak potential from SWV of 74.1 μM acetaminophen at different pH buffers plotted vs. pH. **F** SWVs of 74.1 μM acetaminophen in different pH buffers. **G** CV of 74.1 μM acetaminophen at different scan rates. **H** Oxidation and reduction peak currents (I_a and I_c) plotted vs. the square root of scan rate. Anodic current is plotted as positive and cathodic is negative.

the highest enhancement in peak current in both the CV of ferrocyanide-ferricyanide, and the SWV of acetaminophen. Measurements from this point on are performed with the SSf-modifed with carbon ink that is doped with AuNPs (abbreviated as C-Au-SSf). To optimize the concentration of AuNPs in the carbon ink, we tested four different concentrations of AuNP solution per 3.5 grams of ink: 5 μL, 10 μL, 20 μL, and 30 μL. SWVs in 84 μM acetaminophen in pH 7 buffer were measured with c-AuNP-SSf with different AuNP concentrations (Supplementary Fig. 2), and the 20 μL amount resulted in the sharpest peak and a high peak intensity. This AuNP ink concentration was used for the fabrication of sensors presented beyond this point to achieve high sensitivity, while conserving the amount of nanomaterials used for device fabrication in order to maintain a low cost.

Characterization of surface functionalization

Figure 2A shows the SEM image of pristine SSf. The aligned thread fibers have a size of 13.8 ± 0.8 μm and are twisted together to form an approximately 500 μm fiber bundle. The void space between the thread fibers is adequate for the conductive ink to infuse, while providing mechanical support, lightness, portability, and flexibility to our sensing platform. Figure 2B shows the SEM of C-AuNP-SSf, demonstrating consistent infusion of carbon and AuNPs among the fibers, creating an integrated thread with a diameter of 442.5 ± 17.3 μm.

Raman spectroscopy (Fig. 2C) was employed to characterize the carbon ink, as well as the mixture of carbon ink with AuNPs. We obtained the characteristic peaks for carbon-based materials: the D peak at 1358 cm^{-1}, the G peak at 1530 cm^{-1}, and the 2D peak at 2696 cm^{-1}. The G peak suggests the presence of sp^2-bonded carbon atoms arranged in a hexagonal lattice, while the D peak indicates the presence of amorphous carbon as well as defects present in the graphite structure. The I_{2D}/I_G ratio indicates a multilayered graphitic structure in the samples provided[57–59]. We also observed an increase in the I_G/I_D ratio after introducing AuNPs into the carbon ink mix which is a phenomenon commonly observed in carbon materials containing AuNPs caused by the scattering effect of the nanoparticles[60,61]. Figure 2E shows the electrochemical impedance spectrum (EIS) of the pristine and modified fiber, validating that the modification with the AuNP-doped carbon ink drastically lowers the charge transfer resistance, and facilitates electrochemical analysis at the surface of the modified fiber. SWV measurements were performed in 74.1 μM of acetaminophen, spanning a potential range from 0 to 0.8 V (Fig. 2F). The pristine SSf exhibited the least catalytic activity, whereas the C-AuNP-SSf showed the highest catalytic current.

To determine the electroactive surface area in C-SSf and C-AuNP-SSf, we employed the use of various scan rates in CVs measured in 5.0 mM $[Fe(CN)_6]^{3-,4-}$ (Fig. 3A and C). We measured peak currents at different scan rates, and plotted the values against the square root of the scan rate (Fig. 3B and D). The electroactive surface area (A) can be calculated from the slope of this plot, following the Randles-Ševcík (Equation (1))[62,63]. In this equation, n shows the number of electrons in the electron transfer reaction, F is the

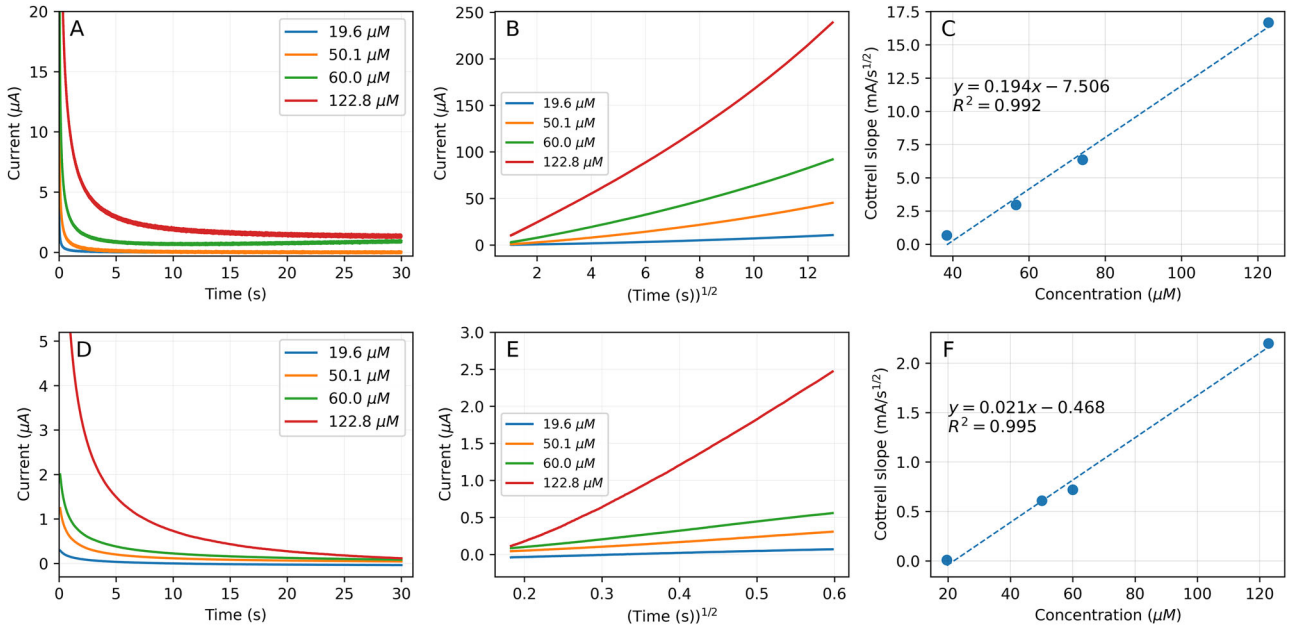

Fig. 4 | Calculation of diffusion coefficient. Chronoamperometric analysis of acetaminophen with varying concentrations in pH buffer 7 (**A**) and undiluted breast milk (**D**), measured at a bias potential of 0.35 V. The Cottrell behavior of chronoamperometric measurements, showing linear relationship of anodic current vs. the reciprocal square root of time ($t^{-1/2}$) in pH buffer 7 (**B**), and milk (**E**). The Cottrell slope plotted vs. concentration of acetaminophen in pH buffer 7 (**C**) and in undiluted breast milk (**F**). All measurements were performed at C-AuNP-SSFf with an external Pt counter electrode, and an Ag-AgCl reference electrode.

Faraday's constant, C is the concentration, D is the diffusion coefficient, v is the scan rate, R is the universal gas constant, and T is temperature.

$$i_p = 0.4463nFAC\sqrt{\frac{nFvD}{RT}} \quad (1)$$

The C-AuNP-SSf had a higher electroactive surface area of 37.5 mm^2 compared to the C-SSf (26.5 mm^2). This enhancement in electroactive surface area is a result of the incorporation of AuNPs into the carbon matrix. In addition to increasing the electroactive surface area, the AuNPs also improve the charge transfer between acetaminophen and the surface of our electrode (Fig. 2E shows the EIS and the charge transfer resistance).

Effect of pH and scan rate on the oxidation of acetaminophen

The pH value of the electrolyte solution is another important factor that can affect the oxidation of acetaminophen and its resultant electrochemical response. Changes in pH can affect the availability of protons in solution which can significantly impact the kinetics of acetaminophen oxidation. The influence of supporting electrolyte pH on acetaminophen was studied using SWV (Fig. 3E, F). Using the Britton-Robinson (B-R) buffer solution, a pH range from 2.5 to 9.0 was tested. As the pH of the solution increased, an indirect correlation with the oxidation peak potential of acetaminophen was observed. Figure 3E shows that the anodic peak potential shifted towards more negative values with increase in pH. This finding suggests the involvement of a proton-electron transfer process in the electrochemical oxidation of acetaminophen at the interface of the sensor (Fig. 1C)[64]. Eq. (2) shows the linear correlation between the anodic peak potential (Epa) and the pH of the solution.

$$E_{pa}\,(mV) = -54.5(pH) + 884.1 \qquad (R^2 = 0.995) \quad (2)$$

The slope of the anodic peak potential vs. pH in Equation (2) was (−54.5 mV pH^{-1}), which is close to the theoretically-expected Nernstian value (−59.2 mV pH^{-1}). This result indicated the oxidation of acetaminophen on the C-Au-SSf electrode involved an equal number of protons and electrons, as demonstrated in Fig.1E. We also investigated the effect of pH on peak current, and achieved the highest peak current at pH 7, which conveniently overlaps well with pH of breast milk (buffered around pH of 7).

The effect of scan rate on the oxidation of acetaminophen at the surface of C-AuNP-SSf electrode was investigated using CVs at various scan rates (Fig. 3G). Both the oxidation and reduction currents increased while increasing the scan rate from 20 to 100 mV s^{-1}. Additionally, a direct linear correlation was observed between the square root of the scan rate and the peak currents (Fig. 3H), indicating a diffusion-controlled process controls the reaction rate (Eqs. (3) and (4)).

$$i_{pa} = 11.1\sqrt{v} - 43.7 \qquad (R^2 = 0.992) \quad (3)$$

$$i_{pc} = -10.5\sqrt{v} + 36.2 \qquad (R^2 = 0.967) \quad (4)$$

In Eqs. (3) and (4), v represents the scan rate, I_{pa} and I_{pc} represent the anodic and cathodic peak currents, respectively, and R^2 is the coefficient of determination.

Measurement of the diffusion coefficient of acetaminophen in breast milk

Given that this study is the first work that explores electrochemical analysis of acetaminophen in human breast milk, we measured the diffusion coefficient of acetaminophen in whole un-diluted breast milk (and buffer as comparison) using chronoamperometry. This method is commonly adopted to examine electrochemical kinetics, and to measure the diffusion coefficient (D) of a species[65].

Figure 4 shows the chronoamperometric responses (voltage held at the oxidation potential of acetaminophen, 0.4 V for buffer and 0.35 V for milk, and current measured over time) at C-AuNP-SSf in various acetaminophen concentrations. The Cottrell's equation (5) explains the dependence of electrical current on parameters such as time (t), Faraday's constant (F), number of electrons in the reaction (n), electrode surface area (A), concentration (C), and diffusion coefficient (D).

$$i = \frac{nFAC_j^0\sqrt{D_j}}{\sqrt{\pi t}} \quad (5)$$

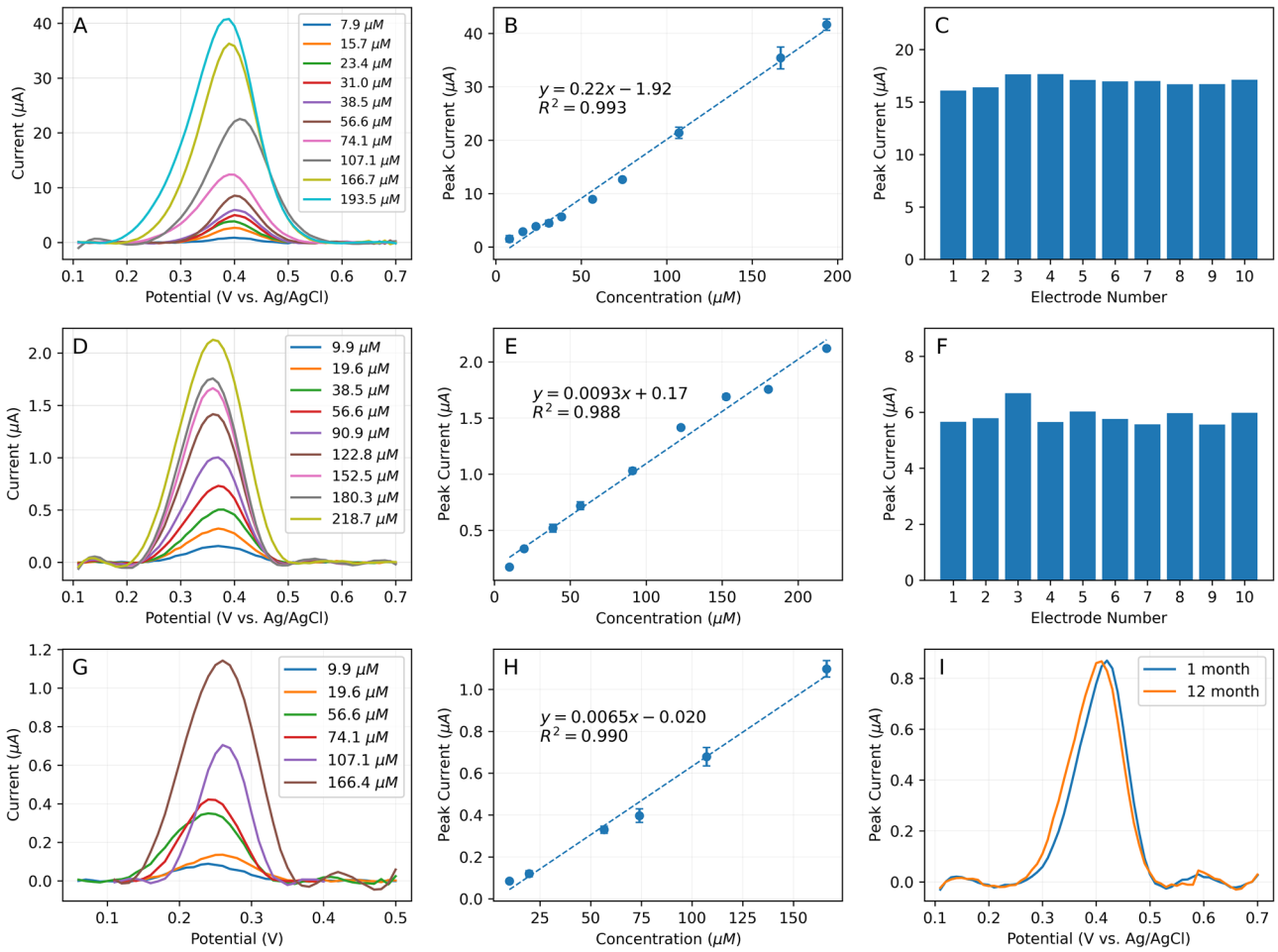

Fig. 5 | Electrochemical measurements in milk. A SWVs in pH 7 buffer, measured with C-AuNP-SSf (external reference and counter electrode) at different concentrations of acetaminophen. **B** Linear relationship of peak current and acetaminophen concentration (measurements in pH buffer 7). **C** Reproducibility of measurements with C-AuNP-SSf (external reference and counter electrode) in pH buffer 7, at 74 μM acetaminophen. **D** SWVs in 6-month milk, measured with C-AuNP-SSf (external reference and counter electrode) at different concentrations of acetaminophen. **E** Linear relationship of peak current and acetaminophen concentration (measurements in 6-month milk). **F** Reproducibility of measurements with C-AuNP-SSf (external reference and counter electrode) in 6-month milk, at 74 μM acetaminophen. **G** SWVs in 6-month milk, measured with C-AuNP-SSf (Ag-plated yarn as reference electrode and pristine SSf as counter electrode) at different concentrations of acetaminophen. **H** Linear relationship of peak current (measured with fully-yarn-based system) and acetaminophen concentration (measurements in 6-month milk). **I** SWVs measured with fully yarn-based system in one-month and 12-month milks containing 74.10 μM acetaminophen.

Figure 4B and E show the expected Cottrell behavior, where the anodic current exhibits linear dependence on the reciprocal square root of time (B is pH buffer of 7, and E is milk). The slope of current vs. $t^{-1/2}$ was then plotted vs. concentration in Fig. 4C and F (C is buffer and F is milk), allowing for calculation of the diffusion coefficient in each matrix. The measured D values for acetaminophen at C-AuNP-SSf in pH buffer and milk solutions were 2.26 x 10^{-5} and 2.75 x 10^{-7} cm^2 s^{-1}, respectively. The observed decrease in the diffusion coefficient value in milk is attributed to the complexity of its constituents. Milk contains many components such as proteins, lipids, carbohydrates, and minerals, any one of which can retard acetaminophen molecules and restrict their diffusion to the electrode's surface.

Calibration and validation of C-AuNP-SSf in buffer and milk

In this section, we evaluate the sensitivity, selectivity, and accuracy of analysis with the C-AuNP-SSf in pH buffer and undiluted whole human breast milk. Calibrations were performed using SWV to lower the effect of capacitive current. Acetaminophen's peak concentration (C_{max}) in breast milk ranges from 66.1 to 99.1 μM[66]. We calibrated the C-AuNP-SSf in a concentration range of 10 μM to 190 μM to fully capture the physiologically-relevant and potentially toxic concentrations of acetaminophen in milk. Figure 5A shows the SWVs of acetaminophen in a buffer with pH 7, validating that peak current increases at higher concentrations of acetaminophen. Fig. 5B establishes a linear correlation between peak current and concentration of acetaminophen in buffer from 8 to 194 μM. A limit of detection (LOD) of 1.4 μM, and a limit of quantification (LOQ) of 4.5 μM were achieved. The reproducibility and repeatability of the fabricated C-AuNP-SSf electrodes were assessed by examining the response to the same concentration of acetaminophen across 10 different electrodes (Fig. 5C). The relative standard deviation (RSD) was 2.92%, indicating a high degree of consistency and reliability in the platform's performance.

To evaluate the performance of the C-AuNP-SSf in breast milk, the SWV was measured in un-diluted milk (Fig. 6A–C). The milk was then spiked with 74 μM acetaminophen and SWVs were measured again, demonstrating that the acetaminophen oxidation peak appears in the spiked samples (Fig. 6A–C). The milk matrix appears to lower sensitivity to acetaminophen, likely by blocking of the electrode surface; however, none of the milk components produce peaks that directly overlap with the acetaminophen peak. The C-AuNP-SSf platform is able to measure acetaminophen directly in un-diluted milk without any interference from milk components, and without the need for any sample preparation, creating a

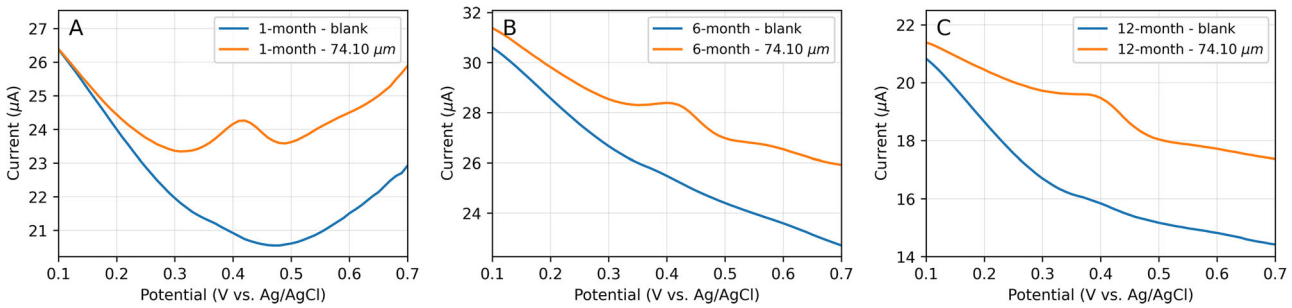

Fig. 6 | Selectivity studies. A SWVs, measured with C-AuNP-SSf (external reference and counter electrode), at 74.1 μM acetaminophen in one-month, **B** 6-months, and **C** 12-month milk samples. The blue traces show the background current without any acetaminophen, and orange traces show the measurement after acetaminophen is spiked in the milk.

Table 1 | Recovery values (n=3) in 1-month and 12-month milk samples

1 month breast milk		12 month breast milk	
Concentration (μ M)	**Recovery (%)**	**Concentration (μ M)**	**Recovery (%)**
19.6	94.6 ± 9.4	9.9	98.4 ± 9.6
74.1	99.9 ± 5.2	74.1	95.9 ± 6.3
137.9	98.9 ± 3.8	193.6	94.6 ± 4.1

Measurements performed with C-AuNP-SSf as working electrode, and external Ag-AgCl reference electrode, and a Pt wire as counter electrode.

powerful technology for at-home analysis of acetaminophen in milk. The composition of milk changes during the period of lactation to best meet the needs of the growing infant[67,68]. To ensure that our analysis is rigorous, and fully captures the complexities of the milk composition at different lactation times, we tested our sensors in milk collected at one month, six months, and 12 months postpartum. Figure 6A–C validates that our platform is capable of analyzing acetaminophen across all milk samples.

Figure 5D shows the SWVs (after baseline correction) for acetaminophen at different concentrations in 6-month human milk (undiluted). A linear relationship between peak current and acetaminophen concentration was achieved (Fig. 5E), in a concentration range of 10 μM to 219 μM. The calculated LOD and LOQ were 2.9 μM and 9.7 μM, respectively. Once the regression model based on 6-month postpartum milk samples was created, we then wanted to determine if we could successfully apply it to milk sampled at one month and 12 months postpartum. These milks were then spiked with acetaminophen, and the C-AuNP-SSf was used to measure a SWV, followed by determination of acetaminophen concentration using the calibration equation established in Fig. 5E for a 6-month milk. Table 1 shows the recovery values, all ranging from 95% to 99%, confirming the feasibility of electrochemical analysis of acetaminophen in breast milk using the developed platform (calibration in individual milk samples is not needed and the same quantification can yield good results across diverse milk samples).

To further evaluate the sensor's reproducibility and repeatability, ten electrodes were tested using similar acetaminophen concentrations in the 6-month breast milk sample (Fig. 5F). The resultant RSD was computed as 5.7%, confirming a good level of consistency and dependability in the sensor's performance across numerous tests. The reproducibility can be enhanced in future work through automated fabrication of sensors, as opposed to manually applying masks for surface functionalization.

Thus far, we have confirmed that the C-AuNP-SSf can successfully measure acetaminophen in undiluted human milk when used as a working electrode. However, all measurements required external counter and reference electrodes, which is not practical for point-of-care and at-home analyses. To ensure a fully yarn-based system can also result in reliable measurements in milk, we calibrated a fully yarn-based system in 6-month milk at different concentrations of acetaminophen. We used the C-AuNP-SSf as a working electrode, a pristine SSf as a counter electrode, and a silver-plated Nylon fiber as a reference electrode. All fibers are low-cost and accessible, ensuring the platform can be fabricated inexpensively. To validate the performance of the fully yarn-based system, we dipped the electrodes in milk for establishing the calibration equation. As shown in Fig. 5G, SWVs can be obtained successfully. The shift in peak position is attributed to a shift in the reference potential. A linear relationship between peak current and acetaminophen was achieved in the range 9.9 μM to 166.4 μM, validating the promise of a fully yarn-based system (Fig. 5H). The three yarn platform showed an LOD of 4.6 μM, and LOQ of 15.4 μM. We also confirmed that the fully yarn-based sensor bundle can effectively measure acetaminophen in one-month and 12-month milk samples (SWVs in Fig. 5I). Comparing the LOD and sensitivity values between an external reference and counter electrode system and a fully thread-based system, the yarn-based system exhibited a slightly higher LOD and slightly lower sensitivity. This can be attributed to the higher resistance of the yarn-based counter and reference electrodes compared to the traditional external electrodes. Despite this slightly worsened performance, the LOD and linear range of the fully thread-based system is sufficient for measurements in the physiologically expected concentration of acetaminophen in milk.

Integrated yarn sensor measurements

After confirmation of sufficient sensitivity, selectivity, and response range of the three-electrode yarn-based system, which includes a C-AuNP-SSf working electrode, an SSf counter electrode, and an Ag-plated yarn reference electrode, we aimed to develop a scalable, cost-effective integrated sensor platform. We utilized embroidery to create a flexible, fully yarn-based sensor array using a commercially available embroidery machine.

Embroidery is similar to sewing in that it involves stitching into a fabric. The primary difference is that, instead of joining two pieces of material, it is instead aimed at creating numerous, relatively dense stitches in a single piece of fabric. To prevent the fabric from buckling under the strain of a large number of stitches across a small surface area, two primary measures are taken: (1) fabric is inserted in a hoop to ensure uniform tension, and (2) a temporary fabric is applied at the back of the fabric to increase the integrity of the fabric and stabilize the fabric (commonly referred to as a "stabilizer"). Computerized embroidery involves attaching the aforementioned tension hoop to a computer-navigated arm that executes precise stitching that is reliably reproducible.

We used a non-woven polypropylene textile (contact angle of 85.7 degrees) and increased the hydrophobicity of the fabric by applying a biocompatible waterproofing spray (Scotchguard fabric water shield) to achieve a contact angle of 127.3 degrees. The increased fabric hydrophobicity avoids milk leakage to the back of the sensor array, and also helps in defining the surface area of the working electrode, as fluid only contacts the electrode

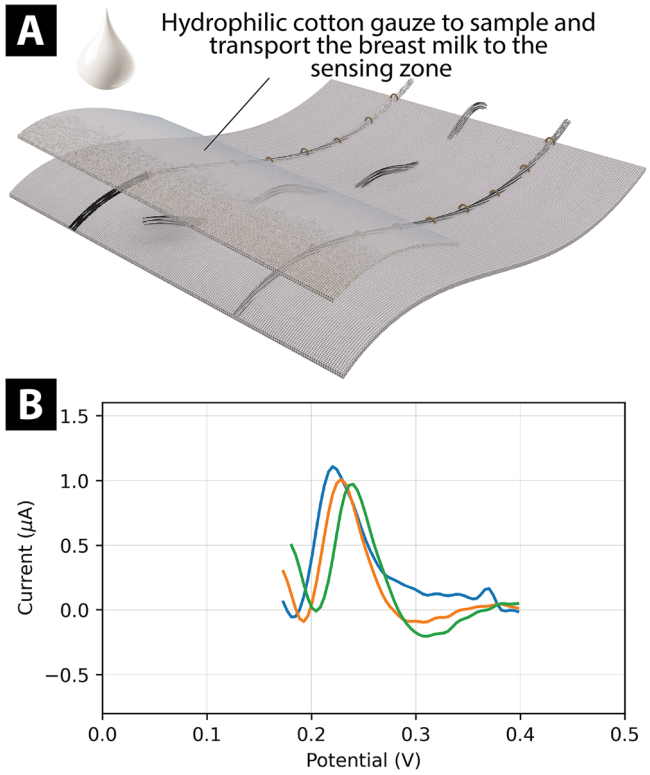

Fig. 7 | Integrated measurements in milk. A Schematic of the integrated yarn-based sensor with a hydrophilic gauze over the sensing zone for improved milk sampling and sensing. **B** SWVs of integrated sensors measured in 166.4 μM acetaminophen in 6-month milk. The three colors show readout from three different sensor patches.

from the top layer. This fabric was then placed in the embroidery loop with a water-soluble stabilizer, and attached to the embroidery machine.

To accomplish integration of our electrodes into the fabric, we wound a standard bobbin with the SSf and used it as the lower-thread in a standard lock-stitch configuration (Fig. 7). All conductive threads were used as a bottom bobbin (lower thread) benefiting from the reduction in machining as the lower thread is not forced through the fabric. In the lock-stitch method, an upper thread (100% polyester which was selected for its hydrophobic qualities and reduced likelihood of wicking away precious sample fluid) is fed through a needle which is then pierced through a piece of fabric (final electrode base textile) and a stabilizing fabric (designed to be removed after machining). That upper thread is then locked into place using a separate lower thread (SSf) from the bottom bobbin. The result is a stitch that is more difficult to unravel than a standard running or chain stitch.

We optimized the embroidery settings which included speed, stitch length, and machine tension. As the reproducibility of all electrodes benefited from the use of the slowest speed setting, it was maintained throughout fabrication. We achieved the highest consistency for embroidered steel fibers with a standard 2.5 mm stitch length combined with a tension setting of 35%. In the case of the Ag-plated yarn, a 3.5 mm stitch length was used to lower mechanical stress due to machining. A 75% tension setting was used for the Ag-plated yarn, and two passes of embroidery (up and down) was adopted to keep the filaments compressed together for optimum conductivity and high resilience of the fiber-bundle. After the embroidery of all yarns (SSf as working and counter electrode, and Ag-plated as reference electrode), a laser-cut mask was placed over the sensing patch, to selectively apply the C-AuNP ink on the working electrode (Fig. 1D, picture of embroidered patch in Fig. 5C). Once the ink was dry, a hydrophilic gauze was placed over the working area and secured with a regular stitch, to assist in milk sampling and storing of milk over the sensing area.

Different milk samples with varying amounts of acetaminophen were measured using the patch-integrated electrodes. The peak current exhibited a linear correlation with acetaminophen concentration in the range of 16 μM to 252 μM (Supplementary Fig. 3). The measured sensitivity, defined as the slope of the regression line (0.0054 μA/μM), closely approximated that of the three-yarn sensor immersed in solution (0.0065 μA/μM). Minor variations in sensitivity were attributed to differences in electrode surface area when the working electrode was integrated into the textile matrix.

Human breast milk containing 166.4 μM of acetaminophen was applied on the patch, and SWVs were measured (Fig. 7B). Subsequent recovery values were calculated using the patch electrodes' calibration equation, achieving recovery values of 95.6%, 98.9%, and 111.2%. These promising results provide strong evidence of the effectiveness of the electrochemical platform for the measurement of acetaminophen in breast milk. Beyond acetaminophen detection, this sensor holds potential for monitoring a wide range of biomarkers related to women's health, paving the way for future research and innovation in this field. The flexible, thread-based sensor is envisioned for use as part of a lactation pad, inserted into a nursing bra. Lactation pads are commonly worn inside nursing bras to absorb leaked milk and prevent stains on clothing. After saturation, the pad can be removed, connected to a portable potentiostat to measure acetaminophen in the collected milk, and then disposed of. While this proof-of-concept device represents a significant step toward accessible breast milk analysis, further work is needed to seamlessly integrate the sensor into nursing bras for on-body use. Future iterations could focus on enabling continuous, real-time monitoring directly on the body.

Discussion

The process of childbirth imposes substantial physiological stress, frequently leading to discomfort and pain during the postpartum period. While acetaminophen is recommended to many mothers for management of pain after vaginal or cesarean deliveries, they are often left wondering as to the amount of drug being passed on to their newborn. Current clinical guidelines allow women to breastfeed while taking acetaminophen. While acetaminophen is generally considered safe, even small amounts present in breast milk may impose additional stress on an infant's liver, particularly in premature, ill, or underweight infants, whose systems are already compromised in managing the physiological burden. A pump-and-dump strategy presents a promising alternative to indiscriminately feeding drug-containing milk to an infant. This approach is employed in specific cases to reduce infant exposure to potential irritants in breast milk while maintaining lactation and milk flow. An effective pump and dump strategy requires knowledge of the kinetics of drug release in milk.

Due to high variability from person to person, and for the same individual across the lactation time, it is challenging to estimate the concentration of acetaminophen in milk using the m/p ratio and pharmacokinetics. A more promising and realistic approach is the measure the concentration of acetaminophen in the milk sample that the infant is about to consume. Our electrochemical sensing platform allows for convenient at-home analysis of acetaminophen in milk without the need for any sample preparation. The user can place this flexible patch inside a nursing bra to collect milk or apply the pumped milk directly onto the sensing zone. The fiber-based sensors can also be embedded in a lactation pad to create smart lactation pads as reported by us in other work[69,70]. We envision that the user could measure acetaminophen levels right before a feeding to assess the drug content in the milk. Additionally, the user can regularly measure acetaminophen levels in the milk to track its release kinetics, helping to determine the optimal timing for "pump and dump" to ensure safe feeding. Also, this platform will grant clinicians and parents (especially those of children with compromised health) the ability to track both direct and indirect drug exposure to help prevent hepatoxicity.

We believe that the frequent at-home monitoring provided by this device will offer parents and care providers better insight into a neonate's day-to-day drug exposure. We believe this is an improvement upon the current method of relying on infrequent maternal blood draws and m/p conversion ratios. This work explored the first fiber-based electrochemical sensor for measurement of acetaminophen in breast milk, and there are

many future steps to take to ensure successful translation. The flexible yarn-based nature of the sensors allows for their integration in wearable devices in future studies to increase the convenience of sensor use. Portable electrochemical detectors should be developed or existing portable detectors (refs. 71–74) used for the signal readout to ensure users can truly measure at-home at low costs. Clinical studies should be performed to better understand dthe istribution of medications in breast milk for each individual. Our sensing platform can also be expanded to other biomarkers for a complete analysis of important biomarkers and potential contaminants in breast milk.

The new low-cost, textile-based, electrochemical sensor has been developed to measure breast milk's acetaminophen levels across various stages of lactation. We opted for a textile-based sensor due to its inherent durability as well as its ability to remain low-cost, scalable, and discrete with minimal packaging and storage requirements. A stainless steel yarn was specifically used for sensor fabrication to its biocompatibility, high conductivity (resistivity of 10 Ohms per foot), and durability this thread. We applied a conductive carbon ink doped with gold nanoparticles on a portion of the working electrode to enhance its electrocatalytic activity towards acetaminophen and to increase the electrode surface area. This modified steel fiber showed excellent sensitivity and selectivity for the measurement of acetaminophen in buffer and breast milk. We demonstrated accurate (less than 10 percent error) measurement of acetaminophen in undiluted whole human breast milk (with a response range of 10 μM to 170 μM), using a flexible embroidered yarn-based sensing platform. This work paves the way for precision breastfeeding in the future and more autonomy for mothers to make decisions about the quality of milk and infant exposure to harmful pharmaceuticals.

Methods

Materials and reagents

Medium conductive 3 ply stainless steel thread was purchased from Adafruit (item P641B). Silver-coated embroidery yarn was purchased from Swicofil. Pellon 541 Wash N Gone 100% PVA Embroidery Stabilizer was purchased from Jo-Ann Fabrics (Item 17311085). Conductive carbon ink was purchased from Sun Chemical (item 321C0814D2). 3M Scotchguard fabric water shield was purchased from Target (item number 003-05-0497). Acetaminophen (product number: 1003009), gold nanoparticles (product number: 808849, 20 nm diameter, 3.27×10^{13} particles/ml), carbon Nanotube, multi-walled, greater than 90% carbon basis (product number: 659258), potassium hexacyanoferrate(II) trihydrate (product number: 1003395970), iron (III) ferrocyanide (product number: 234125), and graphene oxide carboxylic acid enriched (product number: 795542) were all purchased from Sigma-Aldrich. Britton-Robinson buffer (B-R buffer) 0.04 M was made by combining boric acid, phosphoric acid, and acetic acid, and the solution was buffered to pH 2.0 - 9.0 using 0.2 M NaOH. All solutions were freshly prepared and carried out using sterilized deionized water (conductivity of 18.20 MΩ /cm) and analytical-grade chemicals. The platinum wire counter electrode (CHI115) and Ag/AgCl reference electrode (012167) were both purchased from CH Instruments.

This study was conducted in accordance with the ethical principles of the Declaration of Helsinki. The use of de-identified human breast milk samples was reviewed and approved by the University of Southern California Institutional Review Board (IRB) under study protocol HS-23-00356. The IRB granted a waiver of informed consent under 45 CFR 46.104(d)(4) because the research involved only anonymized specimens obtained from a licensed biorepository (Mothers' Milk), and no identifiable private information was accessible to the investigators. All procedures followed institutional and federal guidelines for human subjects research.

Equipment

The sensing platform was fabricated using a Husqvarna Viking Designer Ruby 90 computerized embroidery system and accompanying mysewnet software. Sulky Solvy water soluble embroidery stabilizer was used to stabilize embroidered electrodes without damaging the integrity of conductive textiles. Electrochemical measurements were conducted using a CH Instruments electrochemical workstation (CHI760E). Scanning electron microscopy (SEM) analysis was performed using Nova NanoSEM 450 (FEI, OR, USA), using 10 keV electron beam energy and 3 spot size. Raman spectroscopy characterization was performed using the Horiba XploRA Raman Microscope System (Horiba, Japan).

Electrode fabrication

7-cm pieces of stainless steel thread were cut from the spool and masked using low-tack adhesive tape, leaving 1 cm of exposed thread at the tip. The yarns were secured to a plastic backing, and a laser-cut mask was applied over the yarns, leaving 1 cm exposed at the tips. The ink was prepared by hand mixing 3.5 g of the commercial carbon ink with 20 μL of stated nanoparticle inks (AuNP, GO, MWCNT) for 45 minutes. This ink was then painted onto the 1 cm exposed tip of SSfusing disposable round-tipped clean room swabs. The laser-cut mask was removed prior to drying of the ink, and sensors were left to dry for 24 hours in the fume hood at room temperature.

For embroidery, a non-woven polypropylene fabric was treated using canned 3M waterproofing spray. The material was placed in the hood while the can was held upright and 6 inches away from the fabric. Light, overlapping layers of the product were applied in two coats, with 20 minutes to dry in the hood in between coating applications. Once both sides of the fabric had been treated, it was left to dry overnight in the fume hood. The waterproofed fabric was then placed in a standard 120 x 120 mm embroidery hoop with a commercially available water-soluble material made of 100% polyvinyl alcohol used as an embroidery stabilizer.

The hoop was placed into the computerized embroidery arm of a Viking Designer Ruby 90 computerized embroidery machine, with the accompanying MySewNet software used for electrode design. All conductive threads were incorporated via the bottom bobbin with a 100% polyester all-purpose thread serving as the upper thread in the lock-stitch. Stainless steel working and counter electrodes were single-stitched at the lowest speed setting with a stitch length of 2.5 mm and a tension setting of 35. The reference electrode using Swicofil Silver thread was double-stitched at the lowest speed with a 3.5 mm stitch length and a tension setting of 75.

The silver yarn (reference electrode) was placed between the two steel fibers (working and counter electrodes). This orientation enabled more consistent embroidery, as the stitching methods for the steel and silver yarns differed. The stiffer steel fiber required securing with a loop stitch, while the more flexible silver yarn could be attached using a standard stitch. By spacing the two steel fibers apart, we reduced stress on the fabric, enhancing its durability. The electrodes were spaced 1 cm from each other.

Upon completion of fabrication, the electrode arrays were soaked in deionized water overnight to dissolve away the stabilizer backing and left to dry in the hood. Three electrode arrays were then cut individually from the larger cloth with a 1cm length of thread left exposed at the base. This 1cm was then taped off using low-tack adhesive and coated with functionalization ink formulations optimized in the protocol above.

Measurements in breast milk

Square-wave voltammetric (SWV) tests were conducted at a frequency of 5 Hz, with a 10 mV step potential and a 40 mV amplitude. For the determination of acetaminophen in breast milk, SWV measurements were initially performed in human breast milk devoid of acetaminophen. Subsequently, different aliquots of a 0.001 M acetaminophen standard stock solution were added to an electrochemical cell containing 5 mL of human breast milk.

Data analysis

The capacitive background current in all voltammetric tests has been corrected using baseline correction methods. Using "pybaselines"[75], an open-source Python library, a polynomial background was fitted to the signal after masking the corresponding peak of acetaminophen. Later, this background is subtracted from the signal[58,76]. SciPy, another open-source Python library for scientific and technical computations, was also utilized for linear regression and creating the calibration curve[77]. The limit of detection (LOD), which represents the smallest detectable concentration, is determined

through Equation (6), wherein (S) signifies the slope obtained from the regression formula, and (σ) denotes the standard deviation of the response.

$$LOD = \frac{3\sigma}{S} \quad (6)$$

Similarly, the limit of quantification (LOQ), which represents the minimum concentration that can be accurately quantified, is calculated using Equation (7). The calculated LOD and LOQ were determined to be 1.4 μM and 4.5 μM, respectively.

$$LOQ = \frac{10\sigma}{S} \quad (7)$$

Data availability

Data is available upon request from the authors.

Received: 5 July 2024; Accepted: 10 June 2025;
Published online: 18 August 2025

References

1. Woodcock, J. *Re: Selection of Acetaminophen for Consideration for Listing by the Carcinogen Identification Committee.* Letter from the FDA (2019).
2. Lee, W. M. Acetaminophen toxicity: a history of serendipity and unintended consequences. *Clin. Liver Dis.* **16**, 34–44 (2020).
3. Ayoub, S. S. Paracetamol (acetaminophen): A familiar drug with an unexplained mechanism of action. *Temperature* **8**, 351–371 (2021).
4. Bronstein, A. C., Spyker, D. A., Rumack Jr, L. R. C. B. H. & Dart, R. C. 2011 annual report of the American Association of Poison Control Centers' National Poison Data System (npds): 29th annual report. *Clin. Toxicol.* **50**, 911–1164 (2012).
5. Schilling, A., Corey, R., Leonard, M. & Eghtesad, B. Acetaminophen: old drug, new warnings. *CCJM* **77**, 19–27 (2010).
6. Nourjah, P., Ahmad, S. R., Karwoski, C. & Willy, M. Estimates of acetaminophen (paracetomal)-associated overdoses in the United States. *Pharmacoepidemiol. Drug Saf.* **15**, 398–405 (2006).
7. Ogilvie, J. D., Rieder, M. J. & Lim, R. Acetaminophen overdose in children. *CMAJ* **184**, 1492–1496 (2012).
8. Stravitz, R. T. & Lee, W. M. Acute liver failure. *Lancet* **394**, 869–881 (2019).
9. Sullivan, J. E. & Farrar, H. C. Fever and antipyretic use in children. *Pediatrics* **127**, e20103852 (2011).
10. Thibault, C. et al. The three w's of acetaminophen in children: Who, why, and which administration mode? *J. Pediatr. Pharmacol. Ther.* **28**, 20–28 (2022).
11. Bryant, A. S. & Miller, R. S. Pharmacologic stepwise multimodal approach for postpartum pain management. *Obstet. Gynecol.* **138**, 507–517 (2021).
12. Niu, H. et al. Therapeutic management of idiosyncratic drug-induced liver injury and acetaminophen hepatotoxicity in the paediatric population: a systematic review. *Drug Saf.* **45**, 1329–1348 (2022).
13. Mazaleuskaya, L. L. et al. Pharmgkb summary: pathways of acetaminophen metabolism at the therapeutic versus toxic doses. *Pharmacogenet. Genomics* **25**, 416–426 (2015).
14. Becker, M. *Individualizing Pharmacotherapy: Genetic factors and co-prescribed drugs affecting pharmacotherapy* (Optima Grafische Communicatie, Rotterdam, 2009).
15. Wilson, J., Brown, R. D., Hinson, J. & Dailey, J. Pharmacokinetic pitfalls in the estimation of the breast milk/plasma ratio for drugs. *Annu. Rev. Pharmacol. Toxicol.* **25**, 667–689 (1985).
16. Tamaki, R. et al. Breast milk concentrations of acetaminophen and diclofenac-unexpectedly high mammary transfer of the general-purpose drug acetaminophen. *BMC Pregnancy Childbirth* **24**, 90 (2024).
17. Montaseri, H. & Forbes, P. B. Analytical techniques for the determination of acetaminophen: A review. *TrAC, Trends Anal. Chem.* **108**, 122–134 (2018).
18. Larsen, L. A., Ito, S. & Koren, G. Prediction of milk/plasma concentration ratio of drugs. *Ann. Pharmacother.* **37**, 1299–1306 (2003).
19. Hervada, A., Feit, E. & Sagraves, R. Drugs in breast milk. *Perinat. Care* **2**, 19–25 (1978).
20. Abduljalil, K., Pansari, A., Ning, J. & Jamei, M. Prediction of drug concentrations in milk during breastfeeding, integrating predictive algorithms within a physiologically-based pharmacokinetic model. *CPT: Pharmacomet. Syst. Pharmacol.* **10**, 878–889 (2021).
21. Beaulac-Baillargeon, L., Auclair, A., Matte, L., Gaudreault, R. & Forest, J.-C. A novel approach for the determination of human milk/plasma ratios: Correlation of in vivo and in vitro paracetamol milk/plasma ratios. *Drug Investig.* **7**, 57–62 (1994).
22. Bitzén, P. O., Gustafsson, B., Jostell, K., Melander, A. & Wåhlin-Boll, E. Excretion of paracetamol in human breast milk. *Eur. J. Clin. Pharm.* **20**, 123–125 (1981).
23. Tertis, M. et al. A novel label-free immunosensor based on activated graphene oxide for acetaminophen detection. *Electroanalysis* **27**, 638–647 (2015).
24. Beitollahi, H., Garkani-Nejad, F., Tajik, S. & Ganjali, M. R. Voltammetric determination of acetaminophen and tryptophan using a graphite screen printed electrode modified with functionalized graphene oxide nanosheets within a Fe_3O_4@ SiO_2 nanocomposite. *Iran. J. Pharm. Res.* **18**, 80 (2019).
25. Campos, A. M. et al. Size control of carbon spherical shells for sensitive detection of paracetamol in sweat, saliva, and urine. *ACS Appl. Nano Mater.* **1**, 654–661 (2018).
26. Gomes, N. O. & Raymundo-Pereira, P. A. On-site therapeutic drug monitoring of paracetamol analgesic in non-invasively collected saliva for personalized medicine. *Small* **19**, 2206753 (2023).
27. Banks, M., Amirghasemi, F., Mitchell, E. & Mousavi, M. P. Home-based electrochemical rapid sensor (hers): A diagnostic tool for bacterial vaginosis. *Sensors* **23**, 1891 (2023).
28. Ong, V. et al. An accessible yarn-based sensor for in-field detection of succinylcholine poisoning. *Chemosensors* **11**, 175 (2023).
29. Amirghasemi, F. et al. Fast (flexible acetylcholine sensing thread): Real-time detection of acetylcholine with a flexible solid-contact potentiometric sensor. *Bioengineering* **10**, 655 (2023).
30. Chen, R. et al. Toward personalized treatment of depression: An affordable citalopram test based on a solid-contact potentiometric electrode for at-home monitoring of the antidepressant dosage. *ACS Sens.* **8**, 3943–3951 (2023).
31. Amirghasemi, F. et al. Lift (a lithium fiber-based test): An at-home companion diagnostics for a safer lithium therapy in bipolar disorder. *Adv. Healthc. Mater.* **18**, 2304122 (2024).
32. Piper, A., Månsson, I. Ö., Khaliliazar, S., Landin, R. & Hamedi, M. M. A disposable, wearable, flexible, stitched textile electrochemical biosensing platform. *Biosens. Bioelectron.* **194**, 113604 (2021).
33. Khaliliazar, S. et al. Woven electroanalytical biosensor for nucleic acid amplification tests. *Adv. Healthc. Mater.* **10**, 2100034 (2021).
34. Glavan, A. C., Ainla, A., Hamedi, M. M., Fernández-Abedul, M. T. & Whitesides, G. M. Electroanalytical devices with pins and thread. *Lab a Chip* **16**, 112–119 (2016).
35. Liu, X. & Lillehoj, P. B. Embroidered electrochemical sensors on gauze for rapid quantification of wound biomarkers. *Biosens. Bioelectron.* **98**, 189–194 (2017).
36. Alshabouna, F. et al. Pedot: Pss-modified cotton conductive thread for mass manufacturing of textile-based electrical wearable sensors by computerized embroidery. *Mater. Today* **59**, 56–67 (2022).
37. Mo, L., Ma, X., Fan, L., Xin, J. H. & Yu, H. Weavable, large-scaled, rapid response, long-term stable electrochemical fabric sensor integrated into clothing for monitoring potassium ions in sweat. *J. Chem. Eng.* **454**, 140473 (2023).

38. Tang, J. et al. Three-directional knitted fabric sensor made of elastic carbon-based nanofiber yarn with excellent tensile and pressure sensing performance. *Nano Energy* **128**, 109801 (2024).
39. Liu, X. & Lillehoj, P. B. Embroidered electrochemical sensors for biomolecular detection. *Lab Chip* **16**, 2093–2098 (2016).
40. Sinha, A., Stavrakis, A. K.,, Dhanja. & Stojanović, G. M. Textile-based electrochemical sensors and their applications. *Talanta* **244**, 123425 (2022).
41. Manjakkal, L., Dang, W., Yogeswaran, N. & Dahiya, R. Textile-based potentiometric electrochemical pH sensor for wearable applications. *Biosensors* **9**, 14 (2019).
42. Guo, L., Sandsjö, L., Ortiz-Catalan, M. & Skrifvars, M. Systematic review of textile-based electrodes for long-term and continuous surface electromyography recording **90**, 227–244 (2020).
43. Kannaian, T., Neelaveni, R. & Thilagavathi, G. Design and development of embroidered textile electrodes for continuous measurement of electrocardiogram signals. *J. Ind. Text.* **42**, 303–318 (2013).
44. Logothetis, I. et al. Embroidered electrodes for bioelectrical impedance analysis: impact of surface area and stitch parameters. *Meas. Sci. Technol.* **30**, 115103 (2019).
45. Choudhary, T., Rajamanickam, G. & Dendukuri, D. Woven electrochemical fabric-based test sensors (wefts): a new class of multiplexed electrochemical sensors. *Lab Chip* **15**, 2064–2072 (2015).
46. Zhao, Y. et al. Highly stretchable and strain-insensitive fiber-based wearable electrochemical biosensor to monitor glucose in the sweat. *Anal. Chem.* **91**, 6569–6576 (2019).
47. Wang, R., Zhai, Q., An, T., Gong, S. & Cheng, W. Stretchable gold fiber-based wearable textile electrochemical biosensor for lactate monitoring in sweat. *Talanta* **222**, 121484 (2021).
48. Modali, A., Vanjari, S. R. K. & Dendukuri, D. Wearable woven electrochemical biosensor patch for non-invasive diagnostics **28**, 1276–1282 (2016).
49. Possanzini, L. et al. Textile sensors platform for the selective and simultaneous detection of chloride ion and ph in sweat. *Sci. Rep.* **10**, 17180 (2020).
50. Wang, Y. et al. Woven fiber organic electrochemical transistors based on multiwalled carbon nanotube functionalized pedot nanowires for nondestructive detection of potassium ions. *Mater. Sci. Eng.: B* **278**, 115657 (2022).
51. Wang, L. et al. Weaving sensing fibers into electrochemical fabric for real-time health monitoring. *Adv. Funct. Mater.* **28**, 1804456 (2018).
52. Farajikhah, S. et al. 3d textile structures with integrated electroactive electrodes for wearable electrochemical sensors. *J. Text. Inst.* **111**, 1587–1595 (2020).
53. Christie, I., Leeds, S., Baker, M., Keedy, F. & Vadgama, P. Direct electrochemical determination of paracetamol in plasma. *Anal. Chim. Acta* **272**, 145–150 (1993).
54. Zhang, T., Wang, Z., Zhu, A. & Ran, F. Flexible, twistable and plied electrode of stainless steel cables@ nickel–cobalt oxide with high electrochemical performance for wearable electronic textiles. *Electrochim. Acta* **348**, 136312 (2020).
55. Lyu, X., Su, F. & Miao, M. Two-ply yarn supercapacitor based on carbon nanotube/stainless steel core-sheath yarn electrodes and ionic liquid electrolyte. *J. Power Sources* **307**, 489–495 (2016).
56. Wang, Y., Williamson, N., Dawson, R. & Bimbo, N. Electrodeposition of nickel–iron on stainless steel as an efficient electrocatalyst coating for the oxygen evolution reaction in alkaline conditions. *J. Appl. Electrochem.* **53**, 877–892 (2023).
57. Al-Shami, A. et al. Spooc (sensor for periodic observation of choline): An integrated lab-on-a-spoon platform for at-home quantification of choline in infant formula. *Small* **2311745**, 1–16 (2024).
58. Nejad, S. K. et al. Sustainable agriculture with leafs: a low-cost electrochemical analyzer of foliage stress. *Sens. Diagn*. **3**, 400–411 (2024).
59. Wu, J.-B., Lin, M.-L., Cong, X., Liu, H.-N. & Tan, P.-H. Raman spectroscopy of graphene-based materials and its applications in related devices. *Chem. Soc. Rev.* **47**, 1822–1873 (2018).
60. Grebel, H. & Zhang, Y. Raman spectroscopy of active-carbon electrodes when au colloids are placed at the electrolyte/electrode interface. *Chem. Phys.* **579**, 112171 (2024).
61. Akiyama, T. et al. One-step and room-temperature fabrication of carbon nanocomposites including ni nanoparticles for supercapacitor electrodes. *RSC Adv.* **12**, 21318–21331 (2022).
62. Compton, R. G. & Banks, C. E. *Understanding voltammetry,* 3rd edn. (World Scientific, London, 2018).
63. Al-Shami, A., Oweis, R. J. & Al-Fandi, M. G. Developing an electrochemical immunosensor for early diagnosis of hepatocellular carcinoma. *Sens. Rev.* **41**, 125–134 (2021).
64. Compton, R. G., Kätelhön, E., Ward, K. R. & Laborda, E. *Understanding voltammetry: simulation of electrode processes* (World Scientific, London, 2014).
65. Bard, A. J., Faulkner, L. R. & White, H. S. *Electrochemical methods: fundamentals and applications*, 3rd edn. (John Wiley & Sons, Hoboken, NJ, 2022).
66. Berlin Jr, C., Yaffe, S. & Ragni, M. Disposition of acetaminophen in milk, saliva, and plasma of lactating women. *Pediatr. Pharmacol. (N. Y.)* **1**, 135–141 (1980).
67. Allen, J. C., Keller, R. P., Archer, P. & Neville, M. C. Studies in human lactation: milk composition and daily secretion rates of macronutrients in the first year of lactation. *AJCN* **54**, 69–80 (1991).
68. Ballard, O. & Morrow, A. L. Human milk composition: nutrients and bioactive factors. *Pedia. Clin.* **60**, 49–74 (2013).
69. Al-Shami, A. et al. Mom and baby wellness with a smart lactation pad: A wearable sensor-embedded lactation pad for on-body quantification of glucose in breast milk. *Adv. Funct. Mater*. **35**, 2420973 (2025).
70. Mohamed, M. A. et al. Safer breastfeeding with a wearable sensor for monitoring maternal acetaminophen transfer through breast milk. *Device* 100774 https://doi.org/10.1016/j.device.2025.100774 (2025).
71. Ainla, A. et al. Open-source potentiostat for wireless electrochemical detection with smartphones. *Anal. Chem.* **90**, 6240–6246 (2018).
72. Dryden, M. D. M. & Wheeler, A. R. Dstat: A versatile, open-source potentiostat for electroanalysis and integration. *PLOS ONE* **10**, 1–17 (2015).
73. Rowe, A. A. et al. Cheapstat: An open-source, “do-it-yourself” potentiostat for analytical and educational applications. *PLOS ONE* **6**, 1–7 (2011).
74. Lopin, P. & Lopin, K. V. Psoc-stat: A single chip open source potentiostat based on a programmable system on a chip. *PLOS ONE* **13**, 1–21 (2018).
75. Erb, D. pybaselines: A Python library of algorithms for the baseline correction of experimental data. https://github.com/derb12/pybaselines.
76. Jakubowska, M. Signal processing in electrochemistry. *Electroanalysis* **23**, 553–572 (2011).
77. Virtanen, P. et al. SciPy 1.0: Fundamental Algorithms for Scientific Computing in Python. *Nat. Methods* **17**, 261–272 (2020).

Acknowledgements

M. Mousavi acknowledges the 3M Nontenured Faculty Award, Women in Science and Engineering (WiSE) at the University of Southern California, Zumberge Coordination Research Award, and the NIH Director’s New Innovator Award (DP2GM150018). M. Banks, S. Khazaee Nejad, A. Alshami, A. Soleimani, H. Ma, F. Amirghasemi, and V. Ong thank the University of Southern California, Viterbi Graduate Fellowship. All authors would like to extend their deepest gratitude to all of the team at Mother’s Milk for their collaboration and commitment to improving the health of mothers and children everywhere. Finally, a big thank you to Dr. Christina Chambers and the entire team at the University of California San Diego Human Milk Institute. The funders had no role in study design, data collection, data analysis, data interpretation, or writing of the manuscript.

Author contributions

Stated in the manuscript file. "M. A. Mohamed contributed to methodology, data acquisition and analysis, idea conception, writing of manuscript (original draft), and investigation. M. Banks contributed to methodology, investigation, idea conception, and writing of the manuscript (original draft). S. Khazaee Nejad contributed to data analysis, methodology, and visualization and graphics. A. Alshami, A. Soleimani, F. Amirghasemi, and H. Ma contributed to imaging and material characterization, and writing of the manuscript (original draft). V. Ong contributed to data collection and sensor fabrication. M. P. S. Mousavi contributed to methodology, idea conception, writing of manuscript (original draft), investigation, and funding acquisition. All authors contributed to the review and editing of the manuscript."

Ethics approval and consent to participate

This study was conducted in accordance with the ethical principles of the Declaration of Helsinki. The use of de-identified human breast milk samples was reviewed and approved by the University of Southern California Institutional Review Board (IRB) under study protocol HS-23-00356. The IRB granted a waiver of informed consent under 45 CFR 46.104(d)(4) because the research involved only anonymized specimens obtained from a licensed biorepository (Mothers' Milk), and no identifiable private information was accessible to the investigators. All procedures followed institutional and federal guidelines for human subjects research.

Competing interests

Corresponding PI Maral Mousavi is an associate editor at npj Women's Health. She was not involved in the review or editorial process for this manuscript. This manuscript underwent independent handling by another editor.

Consent for publication

All authors have read and agreed to the published version of the manuscript.

Additional information

Supplementary information The online version contains supplementary material available at https://doi.org/10.1038/s44294-025-00088-6.

Correspondence and requests for materials should be addressed to Maral P. S. Mousavi.